HortScience 60(4):587–600. 2025. https://doi.org/10.21273/HORTSCI18377-24

Photosynthetic Characteristics and Leaf Structure of Yellow-leafed *Lilium davidii* Var. *unicolor*

Yong Wang
Plateau Flower Research Centre, Qinghai University, Xining 810016, China, and Key Laboratory of Landscape Plants and Horticulture of Qinghai Province, Xining 810016, China

Yan Wang and Zhiman Zhang
Plateau Flower Research Centre, Qinghai University, Xining 810016, China

Jinhua Tian, Daocheng Tang, and Nan Tang
Plateau Flower Research Centre, Qinghai University, Xining 810016, China, and Key Laboratory of Landscape Plants and Horticulture of Qinghai Province, Xining 810016, China

Keywords. chlorophyll biosynthesis, chlorophyll fluorescence parameters, leaf yellowing, photosynthesis

***Abstract. Lilium davidii* var. *unicolor* cotton is a famous edible lily with large-scale cultivation in China. To determine the cause of leaf yellowing in *L. davidii* var. *unicolor*, the photosynthetic characteristics and leaf structure of plants at different yellowing levels were studied. The results revealed that the chlorophyll content in the leaves of *L. davidii* var. unicolor decreased significantly as the degree of yellowing increased. Variation in the content of chlorophyll precursors revealed that in yellow-leafed plants, chlorophyll synthesis was impeded at the stage when coprogen is converted into Proto IX. Compared with those of normal plants, the thicknesses of the leaves, upper epidermis, palisade tissue, and spongy tissue of yellow-leafed plants were significantly lower. Distinct plasmolysis was observed in mesophyll cells. The cytomembrane and tonoplast were damaged. The number of chloroplasts and starch grains in the mesophyll cells of yellow-leafed plants decreased. The volume of chloroplasts also decreased, and structural damage occurred. Granum lamella failed to stack into granum, which led to a decrease in or disappearance of granum thylakoid. The variation in chloroplast structure and the reduction in chlorophyll content led to a further decrease in photosynthesis in yellow-leafed *L. davidii* var. *unicolor* plants. The photosynthetic parameters [net photosynthetic rate (Pn), stomatal conductance (Gs), transpiration rate (Tr)] and chlorophyll fluorescence parameters [maximum quantum efficiency of photosystem II (PSII) (F_v/F_m), photochemical quantum yield of PSII [Y(II)], and electron transport rate (ETR)] decreased significantly. The Fv/Fm, Y(II), ETR, and photochemical chemical quenching were significantly positively correlated with Pn, Gs, and Tr, but highly negatively correlated with intercellular CO_2 concentration (Ci) and vapor pressure saturation deficit (VPD). The results of this study provide important information for further studies of the response mechanism of plants to leaf yellowing. In addition, this study provides a theoretical basis for the prevention and recovery of yellow-leafed plants, which are important for increasing the yield and quality of *L. davidii* var. *unicolor* bulbs.**

Lilium davidii var. *unicolor* cotton, which belongs to the genus *Lilium*, is one of the most important edible lilies. Bulbs of *L. davidii* var. *unicolor* have both edible and medicinal value. Therefore, it is used as a special vegetable in China and can be eaten fresh or cooked (Tang et al. 2021). Its bulbs can help strengthen the immune system because they are rich in nutrients such as starch, dietary fiber, vitamins, and various bioactive substances (You et al. 2010; Zhang et al. 2010). *L. davidii* var. *unicolor* has a long cultivation history in China and is propagated mainly by bulb division. With the extension of cultivation time and expansion of production areas, the yellowing phenomenon of the plant has increased substantially. The types of yellowing observed include dispersive yellowing and large-scale yellowing. According to the preliminary survey of our research group, at present, dispersive yellowing is common in the major production areas of *L. davidii* var. *unicolor*, whereas large-scale yellowing is becoming increasingly severe. Leaf yellowing of *L. davidii* var. *unicolor* directly causes plant growth restriction, early death, and a reduction in bulb yield and quality, thus dampening the morale of farmers and affecting the development of the *L. davidii* var. *unicolor* industry.

Plant yellowing during the growing season can be divided into two types: pathological yellowing and physiological yellowing (Liu et al. 2018). Pathological yellowing is caused mainly by pathogen infections (Dovas et al. 2002; Maust et al. 2003). Pathogens such as viruses infect roots, leaves, stems, bulbs, and other plant organs, disrupt their normal metabolic processes, and destroy organ structure. This leads to the appearance of leaf yellowing or chlorosis accompanied by cespitose stems and mottled leaves (Fan et al. 2019; Lee et al. 2007; Niimi et al. 2003; Zhang et al. 2015). Physiological yellowing is relatively common in lily production. Unfavorable environmental factors such as a lack or imbalance of nutrient elements, extreme temperatures, drought, flooding, and inappropriate lighting can cause physiological yellowing (Vacek et al. 2009). For example, the successive cultivation of lilies in the same field will cause continuous cropping obstacles, which will lead to growth restriction and plant yellowing. *L. davidii* var. *unicolor* plants that presented yellowing symptoms in the growing season also died earlier than normal plants did. Many studies related to plant yellowing have focused on investigating the causes (Lecoq et al. 1992; Navas-Castillo et al. 2000; Wu et al. 2007) and recovery approaches (Fan and Mattheis 2000). However, few studies have investigated the variations in the physiological and biochemical characteristics of yellow *L. davidii* var. *unicolor* plants.

Leaf color depends on the content, proportion, and distribution of pigments in the leaves (Reinbothe and Reinbothe 1996). Chlorophyll is the dominant pigment in the leaves of most green plants. A decrease in chlorophyll content causes variation in leaf color. Physiological studies of *Chrysanthemum morifolium* have shown that the yellow color of leaves is caused by chlorophyll loss (Shao et al. 2022). Wang et al. (2017) reported that the leaf chlorophyll content in yellow-leafed *Forsythia* cultivars is significantly lower than that in green-leafed cultivars. Zhang et al. (2019) reported that the total chlorophyll and carotenoid contents in yellow leaves of yellow tea plants were significantly lower than those in yellow and green leaves of normal plants. The chlorophyll content not only is an important indicator of yellow plants but also reflects the degree of photosynthesis of the plant. The content of chlorophyll depends on the dynamic balance between its synthesis and degradation (Rüdiger 1997; Yu et al. 2006). Although the biosynthesis pathways of chlorophyll have been clearly studied, its degradation pathway remains incompletely understood (Büchert et al. 2011; Eckardt 2009; Schelbert et al. 2009). The process of chlorophyll biosynthesis in higher plants is a complicated process

Received for publication 5 Dec 2024. Accepted for publication 17 Jan 2025.
Published online 21 Mar 2025.
This work was supported by the Qinghai Province Science and Technology Department (2023-NK-151) and Kunlun Talent Science and Technology Leading Talent plan of Qinghai Province Program.
N.T. is the corresponding author. E-mail: natasha_tn@163.com.

Table 1. Grading standard of *L. davidii* var. *unicolor*.

Levels of yellowing	Chlorophyll content of leaves ($mg \cdot g^{-1}$)	Phenotype
Y0	>2	Whole plant is green
Y1	1-2	One-third of the plant is yellow
Y2	<1	More than two-thirds of the plant is yellow

in which 5-aminolevulinic acid (ALA), porphobilinogen, uroporphyrinogen III (urogen III), coprogen II, protoporphyrin IX (Proto IX), magnesium-protoporphyrin (Mg-Proto), and protochlorophyllide (Pchlide) are important precursors (Eckhardt et al. 2004; Tripathy and Pattanayak 2012). Generally, the first step is the formation of ALA. The ALA molecules are condensed to urogen III, which is oxidatively converted to Proto IX and then forms Mg-Proto and Pchlide (Beale 1999). By analyzing the variation in the contents of chlorophyll and its biosynthetic precursors, it can be preliminarily inferred that the chlorophyll biosynthesis process is normal. Drought stress causes a metabolic imbalance between chlorophyll and its precursors in *Avena sativa*, in which the content of ALA increases while the contents of porphobilinogen, Proto IX, Mg-Proto, and Pchlide decrease (Liu et al. 2022).

Measurements of leaf photosynthesis parameters and chlorophyll fluorescence provide an approach for exploring the photosynthetic capacity and efficiency of plants (Angert 2006). Variations in chlorophyll fluorescence parameters such as minimal fluorescence (F_o), maximal fluorescence (F_m), maximum quantum efficiency of photosystem II (PSII) (F_v/F_m), F_v/F_o, effective photochemical quantum yield of PSII [Y(II)], photochemical chemical quenching (qP), and non-photochemical quenching (qN) are indicators of a plant's photosynthetic capacity. The chlorophyll fluorescence parameters F_v/F_m, Y(II), qP, and qN activities of a yellow leaf mutant of tomato were lower than those of its wild type under different temperature treatments (Ji et al. 2024). Similar variation was also found in yellow 'Cabernet Sauvignon' grapes (Huang et al. 2020). The measurement of parameters such as F_v/F_m is a relatively easy approach used to determine the degree of variation in photosynthesis before a plant presents visible symptoms (Willits and Peet 1999). Generally, the variations in chlorophyll fluorescence parameters signify that plants protect their photosynthetic reaction center by adjusting energy dissipation.

The leaf structure and chlorophyll content of yellow-leafed plants are significantly different from those of green-leafed plants (Xu et al. 2023). Generally, the chlorophyll content of

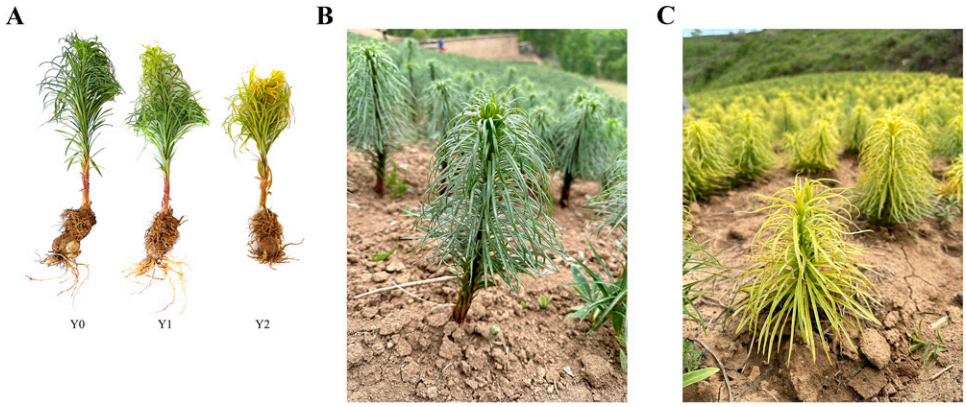

Fig. 1. Phenotype of *L. davidii* var. *unicolor* plant. (**A**) Phenotypes of *L. davidii* var. *unicolor* plants with different levels of yellowing. (**B**) Normal plants in the field. (**C**) Yellow plants in the field.

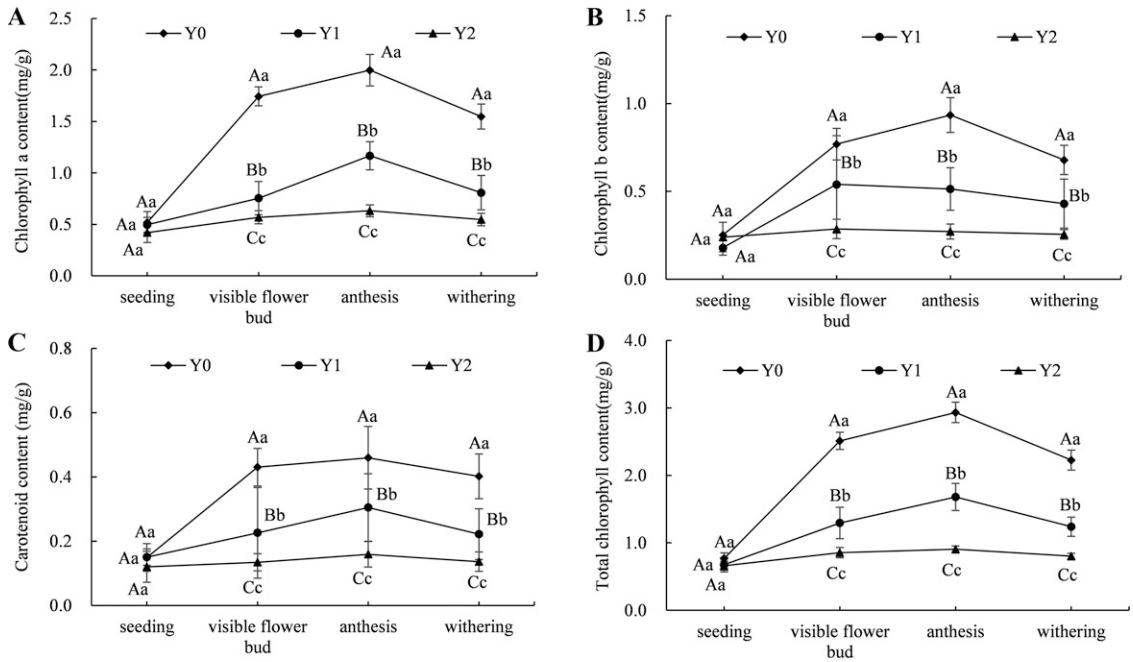

Fig. 2. Variation in the photosynthetic pigments in the leaves of *L. davidii* var. *unicolor*. (**A**) Chlorophyll a. (**B**) Chlorophyll b. (**C**) Carotenoids. (**D**) Total chlorophyll. Different uppercase letters indicate highly significant differences ($P < 0.01$), and different lowercase letters indicate significant differences ($P < 0.05$).

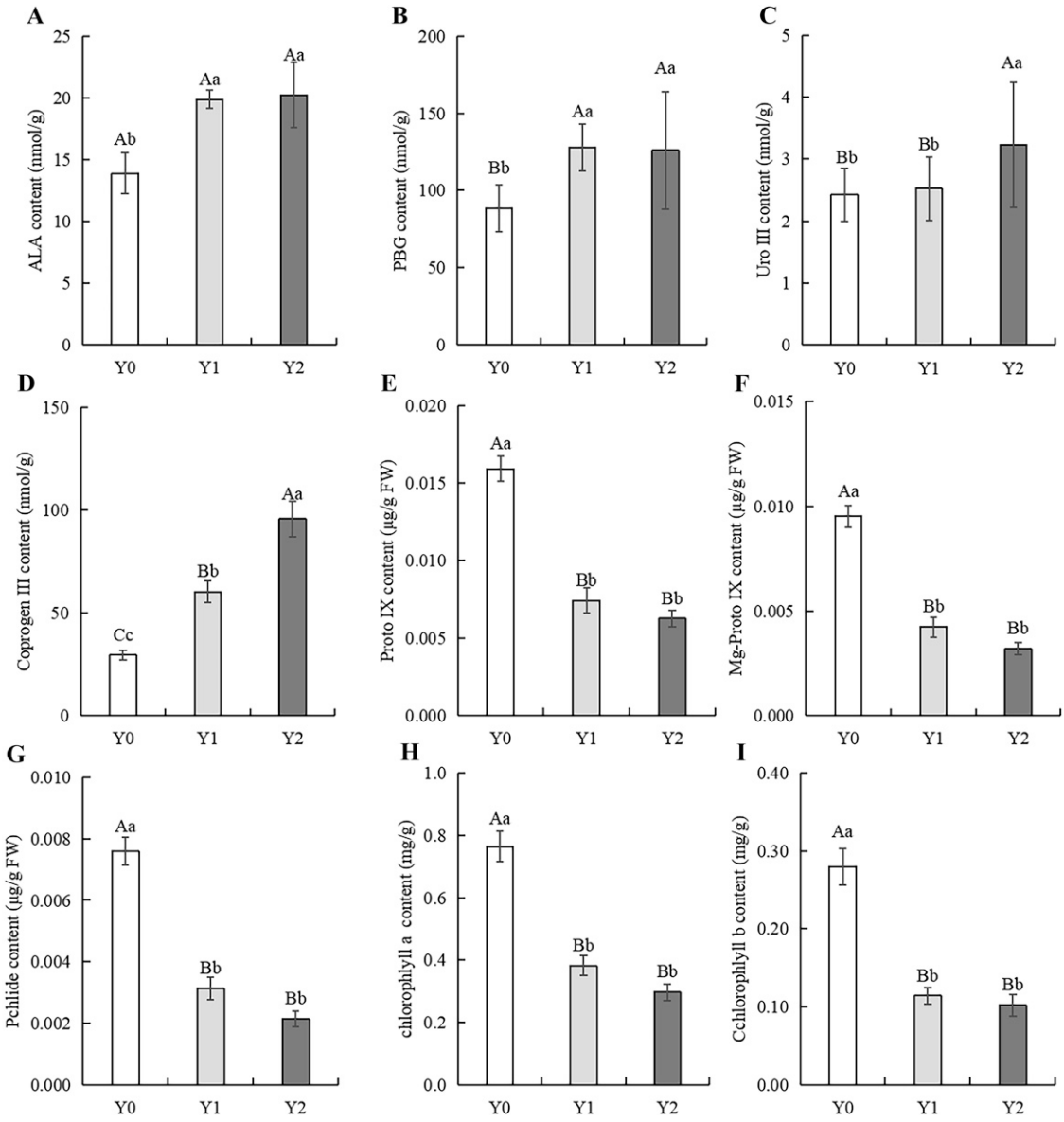

Fig. 3. Contents of chlorophyll synthesis precursors in leaves of *L. davidii* var. *unicolor* of different yellowing grades. (**A**) 5-Aminolevulinic acid. (**B**) Porphobilinogen. (**C**) Urogen III. (**D**) Coprogen III. (**E**) Protoporphyrin (Proto) IX. (**F**) Magnesium protoporphyrin (Mg-Proto) IX. (**G**) Pchlide A. (**H**) Chlorophyll a. (**I**) Chlorophyll b.

yellow-leafed plants is lower than that of green-leafed plants (Wang et al. 2017). A decrease in chlorophyll content usually accompanies abnormalities in chloroplast structure. Zhang et al. (2023) reported defects in the leaf structure of a *Brassica napus* yellow leaf mutant in which mesophyll cells were out of shape and irregularly arranged. The palisade tissue and spongy tissue were loosely arranged. Similar results were reported by Xiao et al. (2013) for *Brassica napus* L. Chang et al. (2019) reported that the leaf microstructure of a tree peony (*Paeonia suffruticosa*) yellow-leaf mutant was similar to that of green leaves. However, there was a significant difference in the chloroplast ultrastructure between the green-leafed and yellow-leafed mutants. The stacks of grana disappeared from the chloroplasts of the yellow-leafed mutant, and only a few stromal thylakoid membranes remained along with clusters of osmiophilic granules. The structure of the thylakoid membranes in these chloroplasts was extremely disordered. Li et al. (2024) reported that the chlorophyll content in the leaves of an eggplant (*Solanum melongena* L.) yellow-leafed mutant was significantly lower than that in green leaves. The membrane structure of the chloroplasts was damaged, and the chloroplasts of the yellow-leafed mutant nearly disintegrated. The grana lamella was uneven and irregularly stacked. Many studies have shown that etiolation can seriously affect the photosynthesis of plants and further cause yield reduction (Chen et al. 2014; Liu et al. 2018; Luo et al. 2022). Although plant yellowing occurs in a large area of *L. davidii* var. *unicolor* production, few studies have been performed to reveal the variations in the physiological and biochemical characteristics of yellow plants. In this study, *L. davidii* var. *unicolor* plants were divided into three different yellowing groups (Y0, Y1, and Y2). Leaf photosynthetic pigments, photosynthesis characteristics, chlorophyll fluorescence parameters, and chlorophyll precursors were determined for plants with different yellowing levels. Moreover, the microstructures of the leaves as well as the ultrastructures of mesophyll cells and chloroplasts have revealed the relationship between leaf structure and yellowing. The aims of this study were to determine the variation in photosynthesis in yellowing plants of *L. davidii* var. *unicolor*, elucidate the relationship between leaf structure and yellowing, and understand the cause of leaf yellowing in *L. davidii* var. *unicolor* at the physiological, biochemical, and cytological levels, which could provide a theoretical basis for further studies of the mechanism of the response to yellowing. In addition, the results of this study could provide a reference for the prevention and recovery of yellow plants, which are important for increasing the

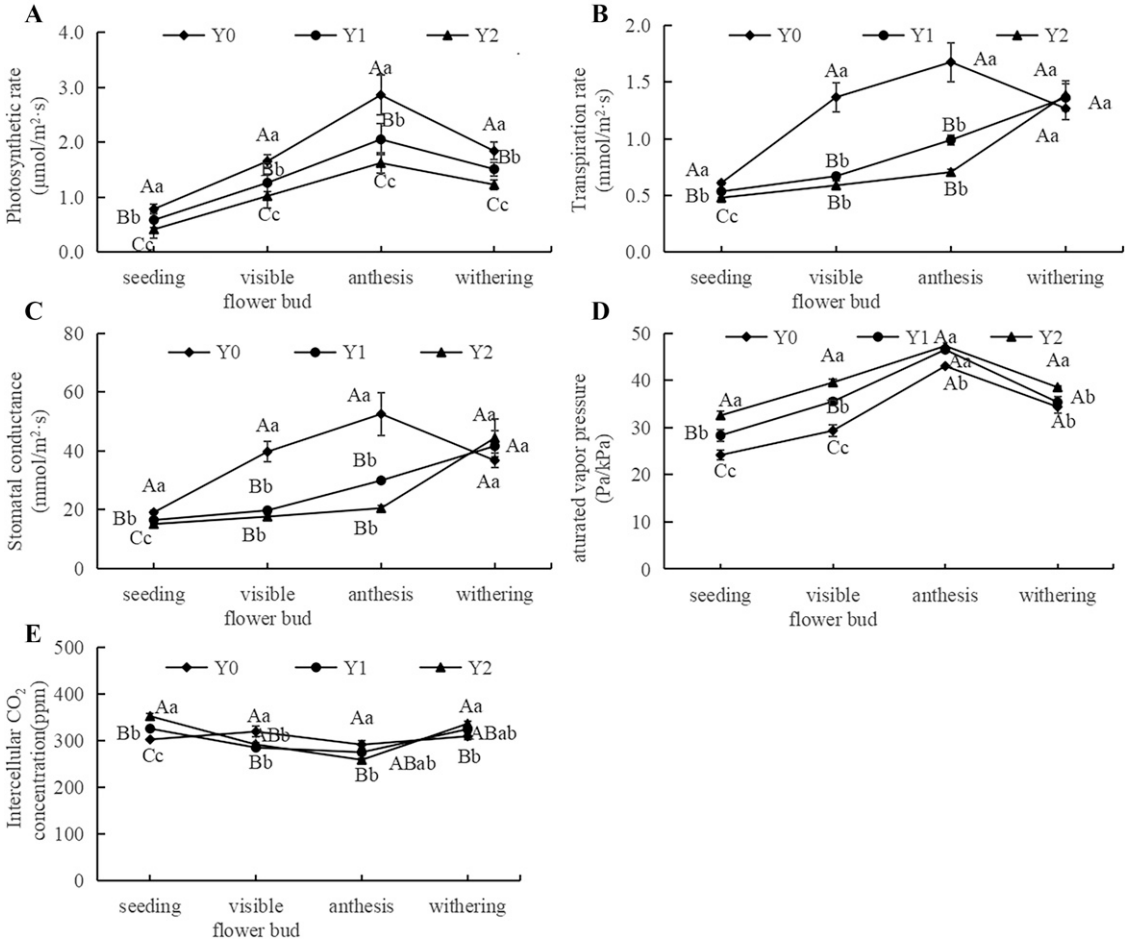

Fig. 4. Influence of yellowing on the photosynthetic parameters of *L. davidii* var. *unicolor* leaves. (**A**) Photosynthetic rate. (**B**) Transpiration rate. (**C**) Stomatal conductance. (**D**) Saturated vapor pressure. (**E**) Intercellular CO_2 concentration.

yield and quality of *L. davidii* var. *unicolor* bulbs.

Materials and Methods

Materials. Bulbs of *L. davidii* var. *unicolor* were planted in Bingling Mountain village of Sanhe town, Ping'an District of Haidong City, Qinghai Province, China (lat. 36°25.8′N, long. 101°59.4′E, altitude 2591.6 m), in Mar 2020. The previous crop of the field was maize. After 1 year of growth, the large-scale yellowing of the plants occurred. In May 2021, *L. davidii* var. *unicolor* plants, which were cultivated for 2 years, were divided into three yellowing groups (Y0, Y1, and Y2) based on the visual observations and the chlorophyll content of the leaves (Table 1, Fig. 1). The plants were transplanted with soil (one bulb per pot) in polyethylene pots with signage in the terrace of the Agricultural and Animal Husbandry Experimental Building of Qinghai University (lat. 36°43.32′N, long. 101°45.2′E, altitude 2310 m) with 30-cm spacing for each pot (23 cm diameter, 13 cm height). The plants were watered thoroughly and covered with a sunshade net for 1 week after transplanting, and routine management was performed once per week. The plants were grown in the same environment and unified cultivation management was applied. The annual average temperature in 2021 was 8.23 °C. The annual precipitation was 476.76 mm. The parameters of leaf photosynthetic characteristics during different growth periods were determined from Apr to Sep 2022.

Determination of chlorophyll content. The chlorophyll content was determined with 80% acetone according to the methods of Arnon (1949). The absorbance (osmiophilic droplet) value was obtained via ultraviolet spectrophotometry (UV-2012C; Unico Instrument Co., Ltd., China) at wavelengths of 665 nm (A665), 649 nm (A649), and 470 nm (A470). The contents of chlorophyll a, chlorophyll b, carotenoids, and total chlorophyll (chlorophyll a+b) were calculated.

Determination of chlorophyll precursors. In Apr 2022, young leaves were collected to measure the content of chlorophyll synthesis precursors. Three individual plants were sampled from each level of yellowing. Three replicates were performed for each plant. The ALA was extracted and quantified according to the methods of Dei (1985). Porphobilinogen, uroporphyrinogen III (urogen III), and coproporphyrinogen III (coprogen III) levels were determined according to the method of Bogorad (1962). The Proto IX, Mg-Proto IX, and Pchlide a levels were determined according to the approach of Liu et al. (2015).

Determination of photosynthetic parameters. A portable photosynthesis measurement system GFS-3000 (Heinz Walz GmbH, Effeltrich, Germany) was used to determine photosynthetic parameters from 9:00 AM to 12:00 AM on a sunny day in Aug 2022. The light intensity was set at 1500 $\mu mol \cdot m^{-2} \cdot s^{-1}$, the flow rate was 750 $m \cdot s^{-1}$, the leaf chamber area was 4 cm^2, and the impeller width was 7. The net photosynthetic rate (Pn), stomatal conductance (Gs), transpiration rate (Tr), intercellular CO_2 concentration (Ci), and water vapor pressure saturation deficit (VPD) were determined. All measurements were performed on the leaves of the middle part of each plant. Three individual plants were measured for each yellowing level. Three replicates were performed for each plant.

Determination of chlorophyll fluorescence parameters. Chlorophyll fluorescence was assessed in vivo via pulse-amplitude modulation (Junior-PAM; Walz, Effeltrich, Germany) according to the methods of Motohashi and Myouga (2015). The plants were dark-adapted for 30 min before the assessment of minimal fluorescence (F_o). The maximal fluorescence

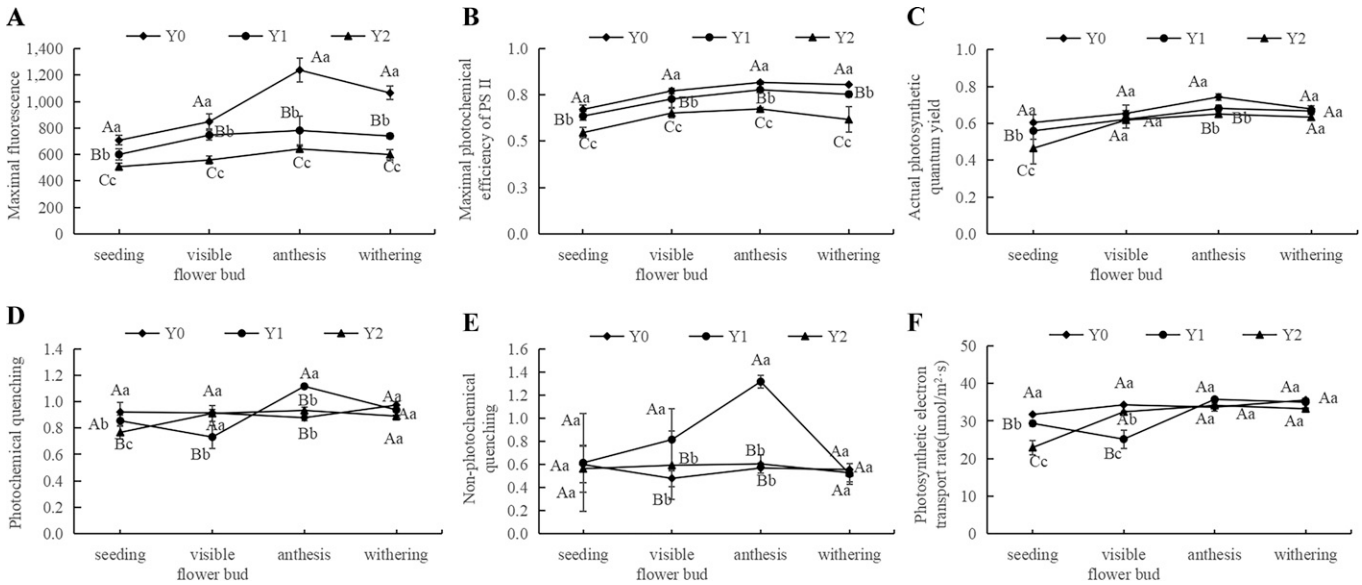

Fig. 5. Influence of leaf yellowing on chlorophyll fluorescence parameters in leaves of *L. davidii* var. *unicolor* of different yellowing grades. (**A**) Maximal fluorescence (Fm). (**B**) Maximal photochemical efficiency of PS II (Fv/Fm). (**C**) Actual photosynthetic quantum yield [Y(II)]. (**D**) Photochemical quenching (qP). (**E**) Nonphotochemical quenching (NPQ). (**F**) Photosynthetic electron transport rate (ETR).

(F_m) was measured with a saturation pulse at 10,000 μmol·m^{-2}·s^{-1} for 0.6 s. The maximum quantum efficiency of PSII (F_v/F_m) was determined as follows: $F_v/F_m = (F_m-F_o)/F_m$. The Y(II), photosynthetic electron transport rate (ETR), qP, and nonphotochemical quenching (NPQ) were obtained under actinic light (125 μmol·m^{-2}·s^{-1}). Three plants were randomly selected from each yellowing level. At least three leaves on the middle part of each plant were selected to determine the chlorophyll fluorescence parameters.

Microstructure of leaves and ultrastructure of leaf chloroplasts. Three plants were randomly selected from each grade of yellowing. The sixth to eighth leaves from the top of each plant were selected for this experiment. To observe the microstructure of the leaf, the middle part of each leaf (5 mm × 5 mm) was sampled. The plant tissue samples were refined, dehydrated, paraffin-embedded, microsectioned, red–solid green-stained, and subjected to other treatments by Nanjing Shuaipu Biological Company. Three different vision fields were randomly selected, and each vision field was repeated three times to measure the leaf thickness, thickness of the leaf main vein, thickness of the upper epidermis, thickness of the lower epidermis, thickness of the palisade tissue, and thickness of the spongy tissue. The ratio of palisade thickness to leaf thickness (CTR) was calculated (Li et al. 2018). The ratio of palisade tissue thickness to spongy tissue thickness (PST) was also calculated (Liu et al. 2018). To observe the ultrastructure of the chloroplast, the middle part of each leaf (1 mm × 1 mm) was sampled, and an ultrathin section was made.

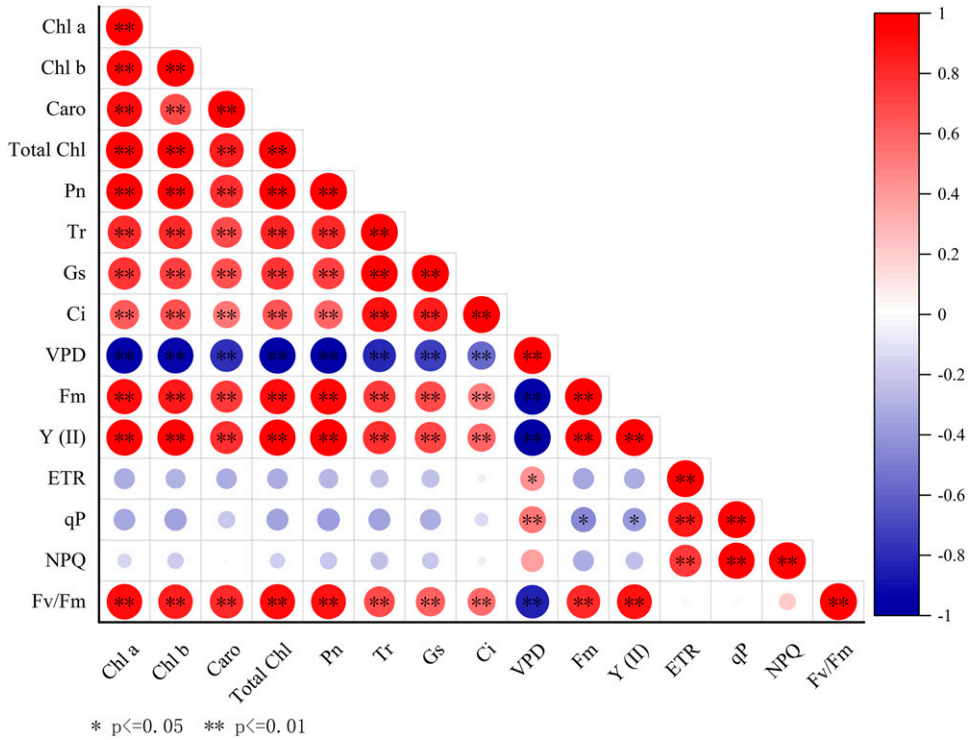

Fig. 6. Correlation analysis of photosynthesis parameters and chlorophyll fluorescence.

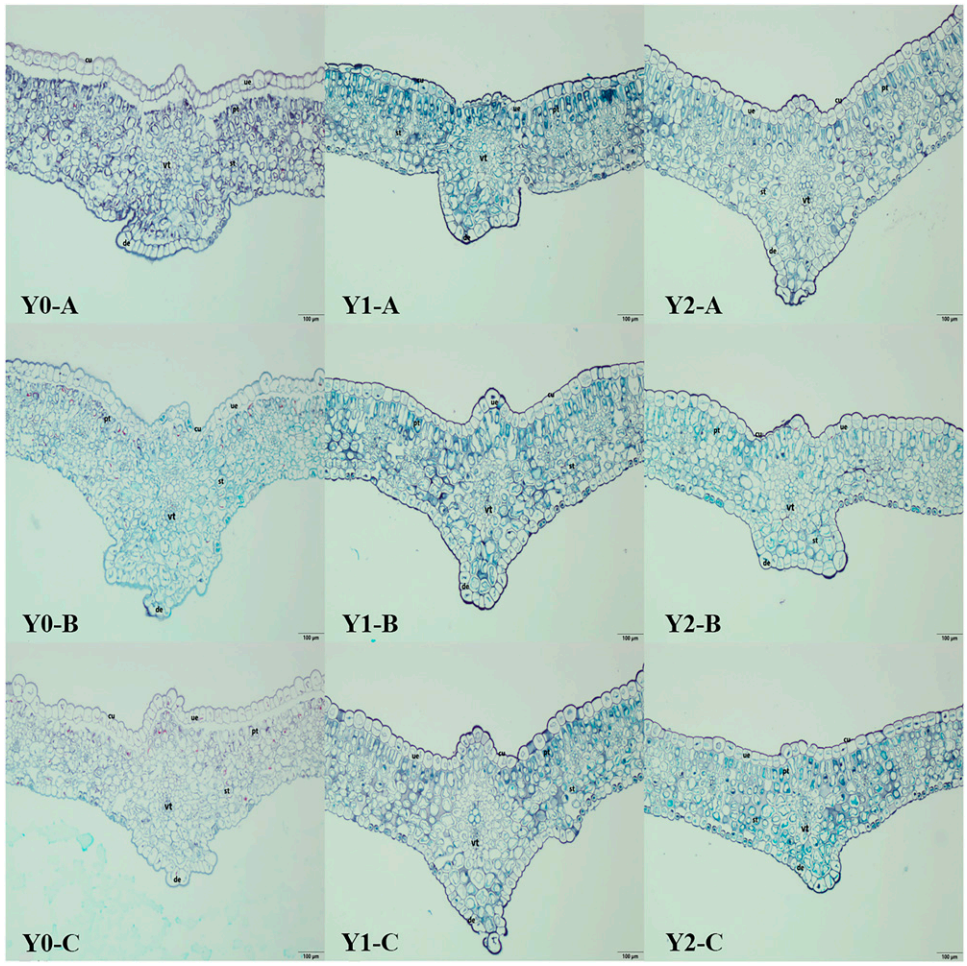

Fig. 7. Leaf anatomical structure of yellow-leafed *L. davidii* var. *unicolor* plants. (**A**) Y0 = seedling stage of Y0; Y1 = seedling stage of Y1; Y2= seedling stage of Y2. (**B**) Y0 = visible flower bud of Y0; Y1 = visible flower bud of Y1; Y2 = visible flower bud of Y2. (**C**) Y0 = anthesis of Y0; Y1 = anthesis of Y1; Y2 = anthesis of Y2.

The dehydrated samples were embedded in epoxy resin and cut into 60- to 80-nm-thick sections. The ultrathin sections were stained with 2% uranium acetate saturated alcohol solution for 15 min, followed by lead citrate for 15 min. Finally, the ultrathin sections were examined under an HT7700 (HITACHI, Tokyo, Japan) electron microscope, and images were taken.

Statistical analysis. An analysis of variance was performed using IBM SPSS Statistics 22, and significant differences between treatments were determined using the least significant difference test at $P < 0.05$. The results of the Pearson correlation analysis and the correlation heatmap were plotted using Origin software (version 9.8.5.204).

Results

Variations in the contents of photosynthetic pigments. The results revealed that in the leaves of normal plants (Y0), the content of photosynthetic pigments was lowest at the seedling stage (Fig. 2). It increased with plant growth and reached its highest value at the anthesis stage. The content of photosynthetic pigments decreased gradually as the plants withered. In the Y1 plants, the variation in the photosynthetic pigment content was the same as that in the Y0 plants. The rate of increase in the content of photosynthetic pigments was lower than that in the Y0 plants. Therefore, the contents of chlorophyll and carotenoids in Y1 plants were significantly lower than those in Y0 plants from anthesis to the withering stage. From the visible flower bud to the withering stage, the photosynthetic pigment content in the leaves of Y2 plants was extremely significantly lower than that in the leaves of Y0 and Y1 plants. No significant variation was observed among the different growth stages.

Variations in the content of chlorophyll precursors. The contents of the chlorophyll precursors ALA, porphobilinogen, urogen III, and coprogen III in yellow plants were greater than those in normal plants (Fig. 3). Proto IX is the oxidative product of coprogen III. Proto IX in yellow-type plants was extremely significantly lower than that in normal plants, which indicated that the metabolic process converting coprogen III to Proto IX was blocked. The contents of Mg-Proto IX and Pchlide in Y1 and Y2 plants were significantly lower than those in Y0 plants.

Influence of leaf yellowing on photosynthetic parameters. The Pn is a key indicator of photosynthesis. As shown in Fig. 4, during the plant growth and development periods, the variation in the Pn of plants of different yellowing grades was similar. From the seedling stage to the anthesis stage, the Pn increased significantly and reached its highest value. As the plants withered, the photosynthetic rates declined rapidly. A comparison of the Pn of different yellow-leafed plants revealed that the Pn of yellow-leafed plants (Y1 and Y2) was extremely significantly lower than that of normal plants (Y0). Furthermore, the Pn of Y2 was extremely significantly lower than that of Y1.

Stomatal conductance represents the degree of stomata opening. It influences plant transpiration, respiration, and photosynthesis. In normal *L. davidii* var. *unicolor* plants, the Gs and Tr were lowest at the seedling stage. Both Gs and Tr increased rapidly as the plant grew and reached their highest values at the anthesis stage. However, the rates of increase in Gs and Tr in yellow plants were lower than those in normal plants. At the seedling stage, the Gs and Tr of Y0 were significantly greater than those of Y1 and Y2. Moreover, the Gs and Tr of Y1 were significantly

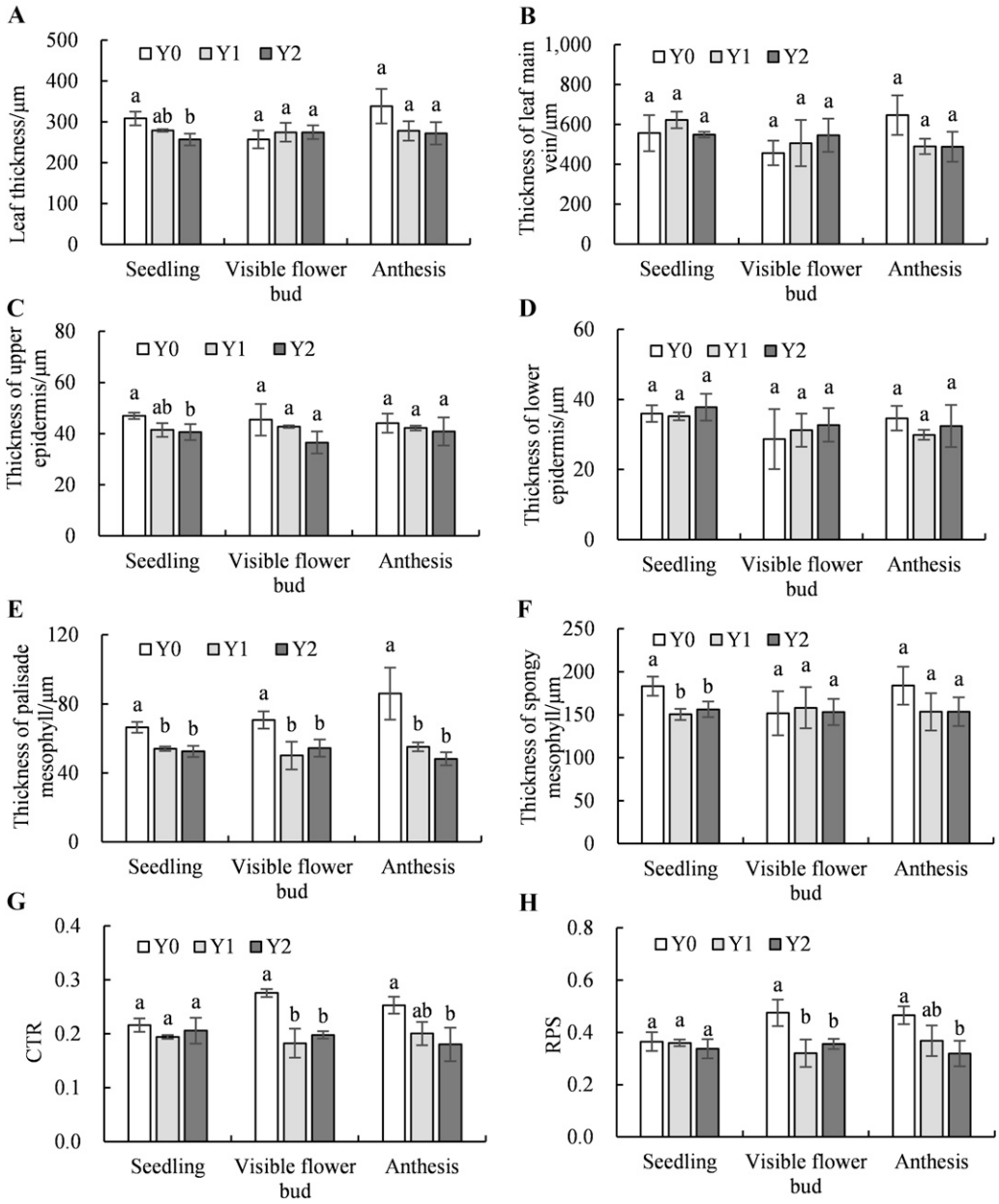

Fig. 8. Parameters of the leaf microstructure. (**A**) Leaf thickness. (**B**) Main vein thickness. (**C**) Upper epidermis thickness. (**D**) Lower epidermis thickness. (**E**) Palisade tissue thickness. (**F**) Spongy tissue thickness. (**G**) The ratio of palisade thickness to leaf thickness (CTR). (**H**) The ratio of palisade tissue thickness to spongy tissue thickness (PST).

greater than those of Y2. At the seedling and anthesis stages, the Gs and Tr of Y1 and Y2 were significantly lower than those of Y0. However, the Gs and Tr of Y1 and Y2 continued to increase until the withering stage. Therefore, no significant variation was detected among plants with different degrees of yellowing at the withering stage.

The variation in the water VPD was consistent with the variation in the Pn in the leaves of *L. davidii* var. *unicolor*. Leaf yellowing induced a significant increase in VPD. From the seedling stage to the anthesis stage, the VPD of the yellow plants was significantly greater than that of the normal plants. At the withering stage, the VPD of Y2 was significantly greater than the VPD of the Y1 and Y0 plants.

The Ci is the ratio of the CO_2 assimilation rate to stomatal conductance. The Ci of normal plants remained relatively stable, whereas the Ci of yellow plants fluctuated significantly. In both the Y1 and Y2 plants, the Ci decreased significantly from the seedling stage to the anthesis stage, but then it increased. The Ci of the Y1 and Y2 plants was significantly greater than that of the Y0 plants at the seedling stage. However, at the seeding and anthesis stages, the Ci of the Y1 and Y2 plants was lower than that of the Y0 plants. At the withering stage, the Ci of Y2 was significantly greater than the Ci of Y0 and Y1.

Influence of leaf yellowing on chlorophyll fluorescence parameters. The results revealed that leaf yellowing significantly influenced the chlorophyll fluorescence parameters (Fig. 5). The F_v/F_m and Y(II) are the maximum and effective photosynthetic efficiencies of PSII, which reflect the potential and effective efficiency of light energy conversion in plants, respectively. During the growth of *L. davidii* var. *unicolor*, the F_v/F_m and Y(II) ratio increased from the seedling stage to the anthesis stage. The F_v/F_m ratio of yellow-leafed plants dramatically decreased to low levels. Significant variation was detected in the plants from the different yellowing treatments. The Y(II) of yellow-leafed plants (Y1 and Y2) was significantly lower than that of normal plants (Y0) at the seeding and anthesis stages. The F_v/F_m and Y(II) of the Y2 plants were the lowest at each stage, indicating that the PSII reaction center was severely damaged (Hu et al. 2023). The ETR of normal plants (Y0) was

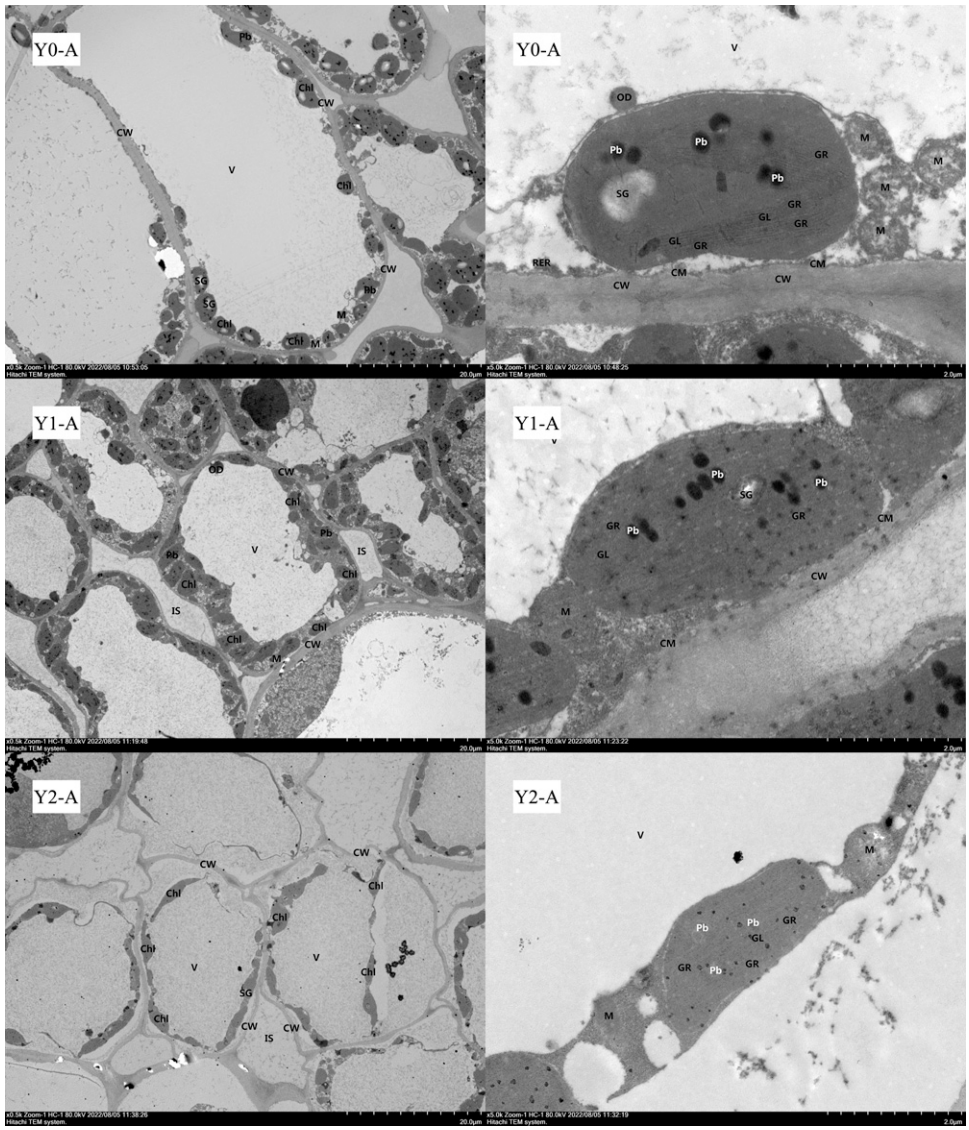

Fig. 9. Ultrastructure of mesophyll cells and chloroplasts of yellow-leafed *L. davidii* var. *unicolor* plants. (**A**) Y0 = seedling stage of Y0; Y1 = seedling stage of Y1; Y2 = seedling stage of Y2. (**B**) Y0 = visible flower bud of Y0; Y1 = visible flower bud of Y1; Y2 = visible flower bud of Y2. (**C**) Y0 = anthesis of Y0; Y1 = anthesis of Y01; Y2 = anthesis of Y2. Chl = chloroplast; CM = chloroplast membrane; CW = cell wall; GL = stroma thylakoid; GR = grana thylakoid; IS = intercellular space; M = mitochondria; N = nucleus; OD = osmiophilic droplet; Pb = plastoglobulus; RER = rough endoplasmic reticulum; SG = starch grain; V = vacuole.

significantly greater than that of Y1 and Y2 plants ($P < 0.05$) at the seedling stage. These findings indicated that plant yellowing significantly reduced the electron transfer rate and potential photosynthetic capacity in the leaves of *L. davidii* var. *unicolor* at the beginning of plant growth.

The decrease in fluorescence reflecting photosynthetic activities is called qP. Like that of the ETR, the qP of the yellow plants was significantly lower than that of the normal plants at the seedling stage. This result indicates that the photochemical conversion efficiency of the leaves decreased when the plants began yellowing. The thermal dissipation of the absorbed light energy of PSII is called NPQ. The results revealed that there was no significant variation in NPQ in plants of different yellowing grades at the seedling stage. The NPQ of Y1 plants increased significantly beginning at the seedling stage and was significantly greater than that of Y0 and Y2 plants at the visible flower bud and anthesis stages. These findings indicate that the heat dissipation efficiency of the Y1 plants was greater than that of the Y0 and Y2 plants.

Correlation analysis of the photosynthetic parameters and chlorophyll fluorescence. The Pn reflects the ability of plants to accumulate organic matter through photosynthesis. It is influenced by the chlorophyll content and chlorophyll fluorescence. A correlation analysis revealed that the Pn was significantly correlated with the contents of chlorophyll a, chlorophyll b, total chlorophyll, and carotenoids (Fig. 6). The photosynthetic parameters were significantly correlated with each other. Strong positive correlations were found between Pn, Gs, Tr, and Ci. Strong negative correlations were found between the VPD and other photosynthetic parameters. Among the chlorophyll fluorescence parameters, strong positive correlations were found between F_m, F_v/F_m, and Y(II). The ETR was significantly correlated with qP and NPQ. A correlation analysis of the photosynthetic and chlorophyll fluorescence parameters revealed that F_m, F_v/F_m, and Y(II) were strongly positively correlated with the photosynthetic parameters Pn, Tr, Gs, and Ci, but highly negatively correlated with VPD.

Microstructure of leaf. The palisade cells of yellow leaves became shorter and smaller, and the spongy cells were no longer full (Fig. 7). The cavity between the spongy cells decreased. The boundary between palisade tissue and spongy tissue is not clear. The leaf microstructure-related parameters revealed that the thickness of the leaf and the palisade tissue and spongy tissue of yellow-leafed plants were significantly lower than those of normal plants at the seedling stage. Compared with that of the control, the leaf

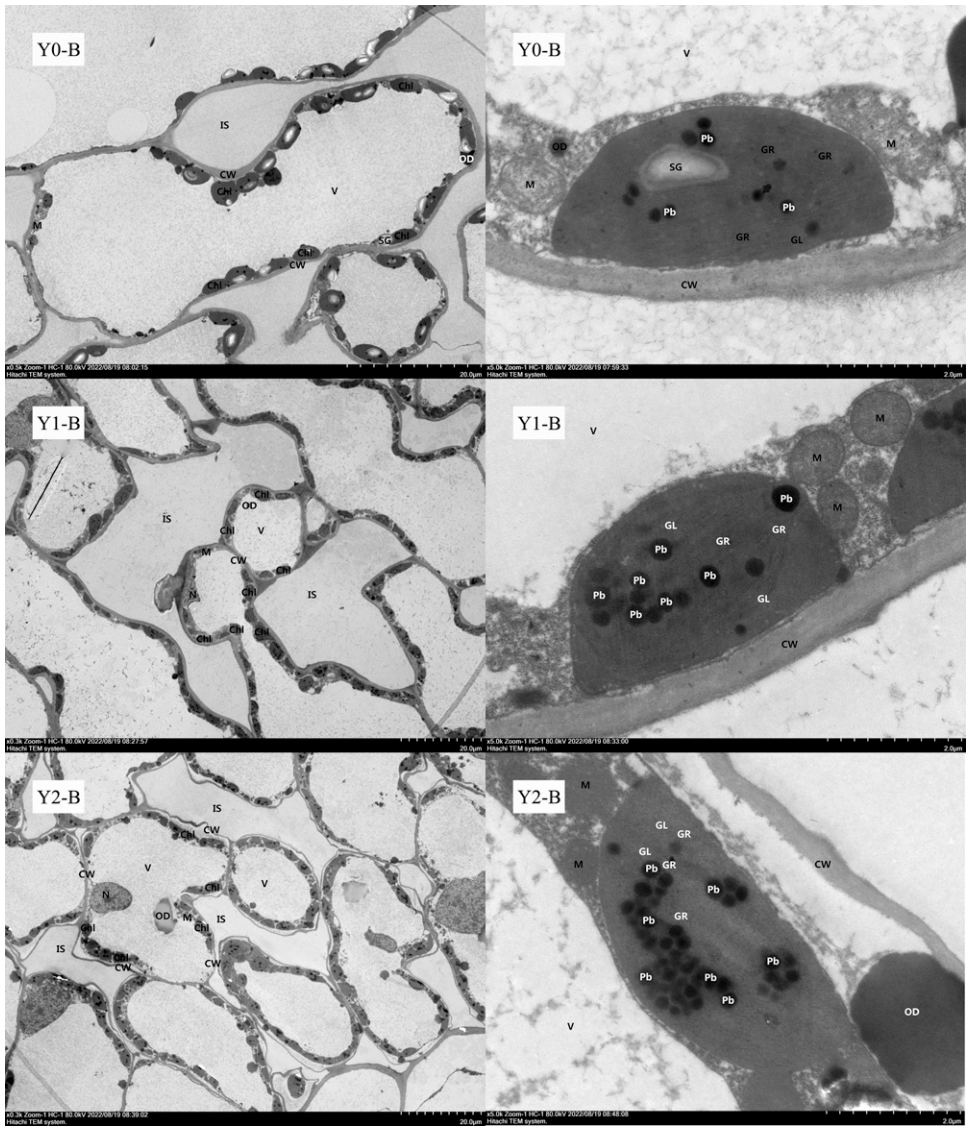

Fig. 9. Continued.

thickness of Y1 and Y2 decreased by 17.9% and 19.6%, respectively, at the anthesis stage. Moreover, the palisade tissue thicknesses of Y1 and Y2 decreased by 35.8% and 43.9%, respectively, compared with that of the control. Compared with that of normal plants, the spongy tissue thickness of yellow-leafed plants decreased by 16.5%. The ratio of palisade thickness to leaf thickness and the ratio of palisade tissue thickness to spongy tissue thickness of yellow-leafed plants were significantly lower than those of normal plants beginning at the visible flower bud stage (Fig. 8).

Ultrastructure of mesophyll cells and chloroplasts. The appearance of mesophyll cells differed among yellow-leafed plants. The thickness of the cell wall was not uniform, and partial damage and atrophy appeared in the cytomembrane. The phenomenon of plasmolysis appears in the cells. Moreover, the number of organelles was lower, the vacuole membrane was damaged, and the number of mitochondrial cristae decreased or even disappeared (Fig. 9).

The number of chloroplasts in the mesophyll cells of yellow-leafed plants decreased, the volume of chloroplasts decreased, and structural damage occurred (Fig. 10). In Y2 plants, granum lamella failed to stack into granum, which led to a decrease in or disappearance of granum thylakoid. At the seedling and anthesis stages, the number of chloroplasts in Y1 and Y2 was lower than that in Y0. The width of chloroplasts in Y2 was significantly lower than that in Y0. The length of chloroplasts in Y1 and Y2 was significantly lower than that in Y0 at the anthesis stage. The number of starch grains in the mesophyll cells of yellow-leafed plants was significantly lower than that in the mesophyll cells of normal plants at all stages. The length and width of starch grains in the mesophyll cells of yellow-leafed plants were significantly smaller than those of starch grains in normal plants at the anthesis stage. The number of plastoglobuli in Y2 was significantly smaller than that in Y1 and Y0 at the seedling stage. However, it was significantly greater than Y1 and Y0 at the visible flower stage. The number of plastoglobuli increased significantly from the seedling stage to the visible flower stage, indicating that obvious accumulation of plastoglobuli occurred in the Y2 plants.

Discussion

Synthesis of chlorophyll in yellow-leafed plants. Changes in plant leaf color are related to the synthesis and degradation of pigments in leaves and the structure and quantity of chloroplasts. The content of photosynthetic pigments is generally lower than that of the corresponding wild type when the leaf color of the plant is yellow, etiolated, or mutated. For example, the pigment content in the yellow area of *Aucuba japonica* is significantly lower than that in the green area (Zhang et al. 2018). In this study, the contents of the photosynthetic pigments chlorophyll a, chlorophyll b, carotenoids, and total chlorophyll in the leaves of yellow *L. davidii* var. *unicolor* plants were significantly lower than those in normal plants during the whole growth and development process. A study of chlorophyll synthesis precursors revealed that the process of chlorophyll synthesis in yellow plants was

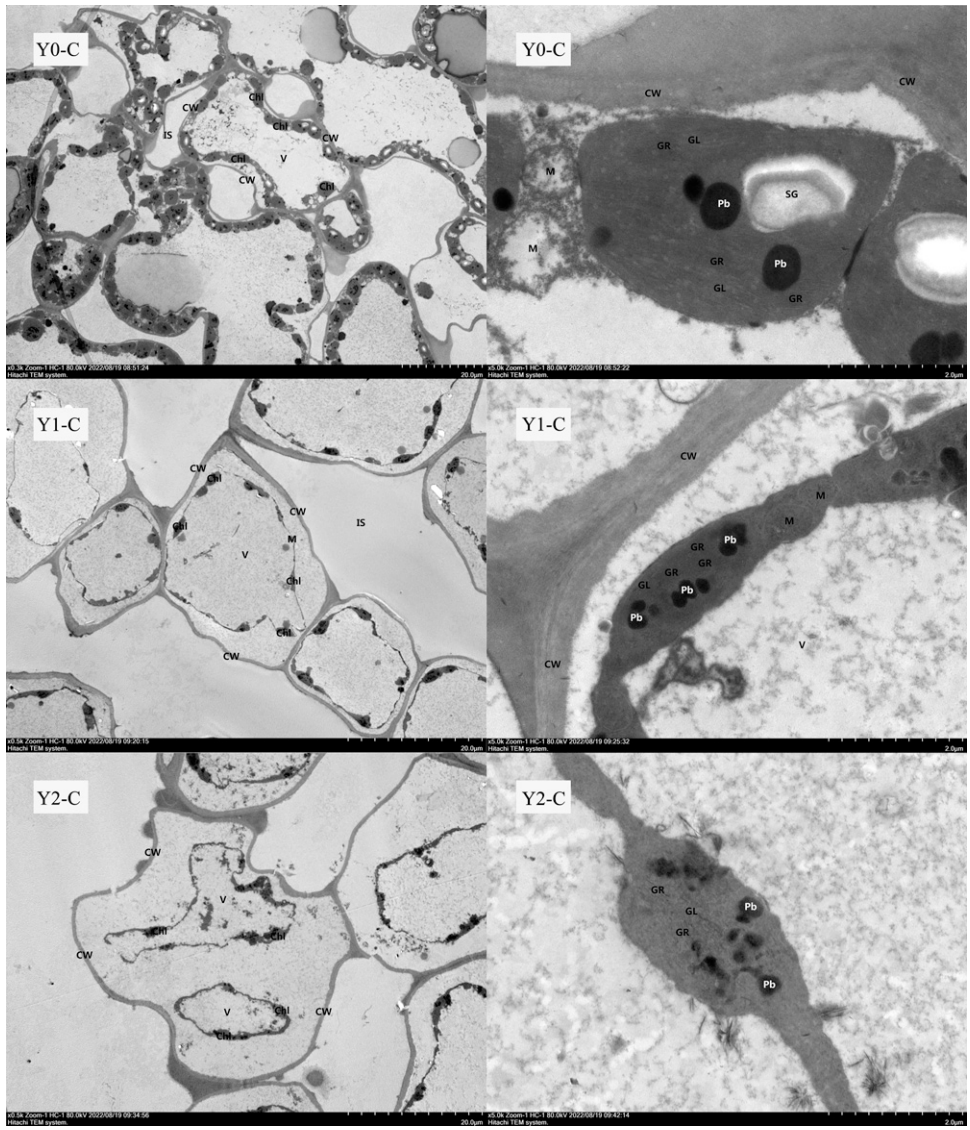

Fig. 9. Continued.

impeded at the step of coprogen III conversion to Proto IX. Blocked synthesis of chlorophyll precursor substances affects the normal synthesis of chlorophyll in leaves, resulting in a lower chlorophyll content, which the leads to changes in leaf color. Currently, blocked sites for chlorophyll synthesis have been identified in a variety of plant leaf color mutants, and the same blocking site has been found in the xantha mutant of *Oncidium* (Wang et al. 2013), the chlorophyll-deficient mutant of *Brassica juncea* (Lv et al. 2010), the variegated leaves of *Iris ensata* (Zeng et al. 2024), and the chlorophyll-less mutant of *Lagerstroemia indica* (Wang et al. 2017). However, different chlorophyll synthesis blocking sites have been found in different leaf mutants of *Cymbidium* hybrids (Zhong et al. 2021).

Leaf anatomy and ultrastructure of chloroplasts in yellow-leafed plants. Yellowing of external morphology occurs under the control of changes in leaf tissue structure and internal cells (Liu et al. 2014). In this study, we observed the leaf anatomical structure of yellow plants of *L. davidii* var. *unicolor* and reported that the leaf thickness, upper epidermal thickness, spongy tissue thickness and palisade tissue thickness of yellow plants were significantly lower than those of normal plants, which is in line with the findings of Sun et al. (2020) and Zhang et al. (2022) on *Forsythia*. Cheng et al. (2022) studied the chloroplast structure and photosynthesis of tomato yellow mutant leaves and reported that compared with those of green leaves, the chloroplast structure of tomato yellow mutant leaves was obviously disrupted, and the photosynthetic capacity was weakened. Xu (2023) reported that more chloroplasts were present in normal plant leaves than in yellow mutant leaves, and significant differences in the arrangement and number of thylakoids were also detected between normal plants and yellow leaf mutants. The thylakoids in normal plants were arranged neatly, concentrated, and numerous, whereas the thylakoids in the yellow leaf mutant were smaller, fewer, thinner, and disordered. In this study, we found that yellowing reduced the number of chloroplasts, which made them smaller, that the basal lamellar system could not stack to form basal granules, and that the lamellar structure of stroma-like vesicles was blurred, which led to a decrease in the photosynthetic capacity of the leaves. In addition, the length of starch grains was significantly reduced in yellow plants, whereas the number of plastid microspheres increased with the increasing degree of yellowing. Starch granules are produced by photosynthetic products that have not had time to be transported out of the chloroplasts, and the decrease in the number of starch granules indicates that the number of photosynthetic products decreases in the leaves of the plants. Plastid microspheres are generally a product of chloroplast-like vesicle membrane degradation, and an increase in plastid microspheres indicates damage to the membrane system of chloroplasts (Prakash et al. 2001; Smith et al. 2000). In terms of whole leaf pulp cells, the greater the degree of yellowing, the greater the degree of plasma wall separation

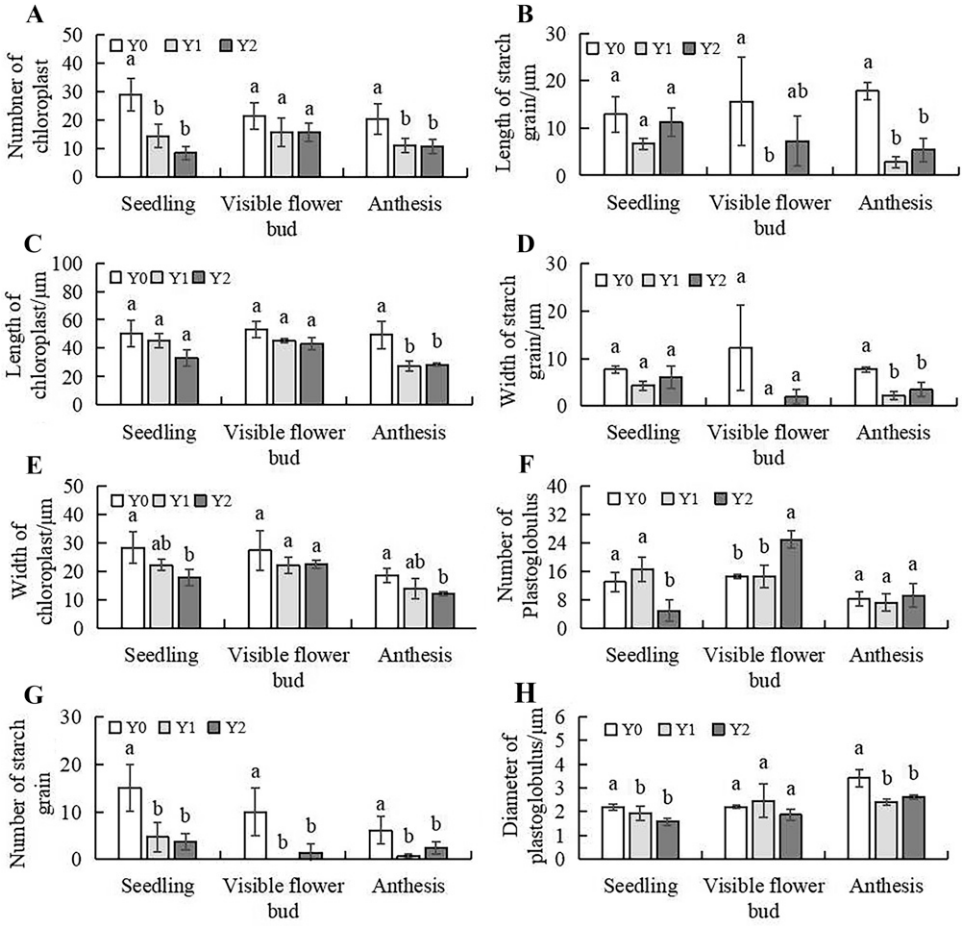

Fig. 10. Parameters of the leaf ultrastructure. (**A**) Number of chloroplasts. (**B**) Length of chloroplasts. (**C**) Width of chloroplasts. (**D**) Number of starch grains. (**E**) Length of starch grains. (**F**) Width of starch grains. (**G**) Number of plastoglobuli. (**H**) Diameter of plastoglobuli.

of the leaf pulp cells, and the cell membrane and vesicle membrane of the leaf pulp cells of the yellow plants exhibited different degrees of breakage, indicating that the yellow plants were no longer able to perform normal osmotic regulation.

Photosynthesis in yellow-leafed plants. The photosynthetic capacity of plants is positively correlated with the content of chlorophyll in leaves. Generally, a decrease in chlorophyll content reduces plant photosynthesis (Sairam and Srivastava 2002). The results of this study revealed that the photosynthetic parameters Pn, Gs, and Tr in yellow-leafed *L. davidii* var. *unicolor* plants were significantly lower than those in normal plants. Similar results were reported for a rice chlorophyll-deficient mutant and *Schefflera odorata* cv. *variegata* (Tan et al. 2019; Wu et al. 2022). Strong positive correlations were found between Pn, Gs, Tr, and Ci, consistent with the results of studies of yellowed grapes and cherries (Huang et al. 2020; Jiang et al. 2022). As an intermediary for photosynthesis in plants, Ci not only is restricted by the CO_2 concentration in the atmosphere but also is influenced by stomatal conductance and photosynthetic consumption in leaves. At the seedling stage of *L. davidii* var. *unicolor*, the Ci of yellow-leafed plants was greater than that of the control. At this time, the photosynthetic rate of yellow-leafed plants was lower than that of normal plants. This result indicates that the consumption of CO_2 by yellow leaves was lower than that by green leaves, which led to higher Ci values. As plants grow, intercellular CO_2 is used. Moreover, the stomatal conductance of yellow leaves was lower than that of green leaves, which means that less CO_2 was absorbed. Therefore, after the seedling stage, the Ci of yellow-leafed plants began to decrease and was lower than that of the control. Generally, a decrease in the photosynthetic rate of plants is caused by "stomatal limitation" or "nonstomatal limitation" (Farquhar and Sharkey 1982; Lawlor 2002). In this study, the GS and chlorophyll contents of yellow-leafed plants were lower than those of normal plants, and the decrease in leaf GS was accompanied by increases in Ci and VPD, which indicate that the decreased photosynthetic rate of *L. davidii* var. *unicolor* was caused by "nonstomatal limitation." Therefore, the low chlorophyll content was the main reason for the decrease in the photosynthetic rate of *L. davidii* var. *unicolor*.

Chlorophyll fluorescence parameters are important indicators that can reflect the photosynthetic activities of plants (Rascher et al. 2000). The F_v/F_m reflects the light energy conversion efficiency of the PSII reaction center. The results of this study revealed that the F_v/F_m and Y(II) of yellow-leafed plants decreased significantly, which was consistent with the findings of a study of *Oryza sativa* L. (Wang et al. 2015). However, the photosynthetic efficiency of the yellow-green leaf mutant (*ygl*) of rice was improved because the light absorbed by the mutant was more efficiently partitioned to photosynthesis (Wang et al. 2022). The F_v/F_m is considered an important parameter for evaluating the level of photosynthetic stress and photoinhibition (Malapascua et al. 2014). Strong positive correlations were found between F_m, F_v/F_m, and Y(II). This finding is consistent with the research results of winter wheat (Jia et al. 2019). Generally, the F_v/F_m of most plants is between 0.80 and 0.85. However, it decreases significantly when stress or injury occurs (Roy et al. 2024). In this study, the F_v/F_m values of the Y1 and Y2 plants were 0.72 ± 0.01 and 0.62 ± 0.01, respectively, which were lower than normal. These findings indicated that yellow-leafed *L. davidii* var. *unicolor* plants were in a state of photoinhibition and that their light energy conversion ability decreased. This finding is consistent with the results reported for *Schefflera odorata* cv. *Variegataso* (Wu et al. 2022), *Sinobambusa tootsik* f. *luteoloalbostriata* (Chen et al. 2019), *Lycopersicon esculentum* (Yang et al. 2018), and grapevines (Shahsavandi et al. 2020). In *L. davidii* var. *unicolor*, the ETR of yellow-leafed plants was

significantly lower than that of the control before flowering. These findings indicated that in the early stage of *L. davidii* var. *unicolor* development, the reduction in the chlorophyll content in leaves reduced the electron transfer rate. Chlorophyll harvests solar energy and drives electrons to transfer light energy to the photosynthetic reaction center (Tanaka and Tanaka 2006). It is believed that a high chlorophyll content could intercept and absorb more light energy (Ort et al. 2015). However, a low chlorophyll content does not always reduce the photosynthetic rate. A study of a pale green-leafed rice mutant suggested that a reduction in chlorophyll content resulted in a significant increase in photosystem II efficiency and ETR (Gu et al. 2017).

Heat dissipation is an important protection strategy when plants are under photoinhibition. Photochemical quenching represents the level of photosynthetic activity of plants, whereas nonphotochemical quenching reflects the ability of plants to dissipate excess light energy into heat, which is the ability of light protection. This study revealed that the NPQ of yellow-leafed plants was greater than that of normal plants. These findings indicate that yellow-leafed plants cannot use excess light energy when the external environment is the same. Therefore, yellow-leafed plants presented better light protection ability, which they achieve by increasing heat dissipation.

Conclusion

The chlorophyll content in the leaves of *L. davidii* var. *unicolor* decreased significantly as the degree of yellowing increased. During the process of chlorophyll synthesis, the conversion step from coprogen to Proto IX is hindered, leading to a decrease in chlorophyll. By observing the microstructure of the leaves and the ultrastructures of mesophyll cells and chloroplasts, abnormal structures were found in yellow-leafed plants. It was deduced that the yellowing of *L. davidii* var. *unicolor* occurred because the chlorophyll synthesis stage was blocked and the chloroplast structure was abnormal. The variation in chloroplast structure and the reduction in chlorophyll content further led to a decrease in the photosynthetic capacity of yellow-leafed *L. davidii* var. *unicolor* plants. The photosynthetic parameters (Pn, Gs, and Tr) and chlorophyll fluorescence parameters (F_v/F_m, Y(II), and ETR) decreased significantly. F_v/F_m, Y(II), ETR, and qP were significantly positively correlated with Pn, Gs, and Tr, but highly negatively correlated with Ci and VPD, which indicated that the PSII reaction center of yellow leaves was damaged, and that the photochemical conversion efficiency of the leaves decreased.

References Cited

Angert AL. 2006. Growth and leaf physiology of monkeyflowers with different altitude ranges. Oecologia. 148(2):183–194. https://doi.org/10.1007/s00442-006-0361-z.

Arnon DI. 1949. Copper enzymes in isolated chloroplasts. Polyphenol oxidase in beta vulgaris. Plant Physiol. 24(1):1–15. https://doi.org/10.1104/pp.24.1.1.

Beale IS. 1999. Enzymes of chlorophyll biosynthesis. Photosynthesis Res. 60(1):43–73. https://doi.org/10.1023/A:1006297731456.

Bogorad L. 1962. Porphyrin synthesis. Methods in Enzymology. 5:885–895. https://doi.org/10.1016/S0076-6879(62)05334-3.

Büchert AM, Civello PM, Martínez GA. 2011. Chlorophyllase versus pheophytinase as candidates for chlorophyll dephytilation during senescence of broccoli. J Plant Physiol. 168(4):337–343. https://doi.org/10.1016/j.jplph.2010.07.011.

Chang QS, Zhang LX, Hou XG, Wang Z, Wang N, Gong MG, Zhang QM, Chen H, Shi ZQ, Deng CC. 2019. The anatomical, physiological, and molecular analysis of a chlorophyll-deficient mutant in tree peony (*Paeonia suffruticosa*). Photosynthetica. 57(3):724–730. https://doi.org/10.32615/ps.2019.049.

Chen J, Sun GM, Shi WQ, Xian HM, Du LQ. 2014. Effects of spraying Fe and organic acids on controlling etiolation and yields of Pineapple. Chin J Trop Agric. 34(06):6–9 + 13. https://doi.org/10.3969/j.issn.1009-2196.2014.06.002.

Chen LL, Xie DJ, Rong JD, Lai JL, Lin XL, Zheng YS. 2019. Effects of photosynthetic pigment content on photosynthetic characteristics of different leaf color phenotypes of *Sinobambusa tootsik eluteoloalbostriata*. Scientia Silvae Sinicae. 55(12):21–31. https://doi.org/10.11707/j.1001-7488.20191203.

Cheng MZ, Meng FY, Mo FL, Qi HN, Wang PW, Chen XL, Liu JY, Ghanizadeh H, Zhang H, Wang AX. 2022. *Slym1* control the color etiolation of leaves by facilitating the decomposition of chlorophyll in tomato. Plant Sci. 324:111457. https://doi.org/10.1016/j.plantsci.2022.111457.

Dei M. 1985. Benzyladenine-induced stimulation of 5-aminolevulinic acid accumulation under various light intensities in levulinic acid-treated cotyledons of etiolated cucumber. Physiol Plant. 64(2):153–160. https://doi.org/10.1111/j.1399-3054.1985.tb02329.x.

Dovas CI, Katis NI, Avgelis AD. 2002. Multiplex detection of criniviruses associated with epidemics of a yellowing disease of tomato in Greece. Plant Dis. 86(12):1345–1349. https://doi.org/10.1094/PDIS.2002.86.12.1345.

Eckardt NA. 2009. A new chlorophyll degradation pathway. Plant Cell. 21(3):700. https://doi.org/10.1105/tpc.109.210313.

Eckhardt U, Grimm B, Hörtensteiner S. 2004. Recent advances in chlorophyll biosynthesis and breakdown in higher plants. Plant Mol Biol. 56(1):1–14. https://doi.org/10.1007/s11103-004-2331-3.

Fan X, Du Y, Cai Y, Zhang Y, Zhao X, Liang J, Yang D, Zhang Q, Zhang X, Zhang W, Xu Y, Zhao K. 2019. Rapid and sensitive detection of cucumber mosaic virus by reverse transcription loop-mediated isothermal amplification. Acta Biochim Biophys Sin. 51(2):223–226. https://doi.org/10.1093/abbs/gmy159.

Fan XT, Mattheis J. 2000. Yellowing of broccoli in storage is reduced by 1-Methylcyclopropene. HortScience. 35(5):885–887. https://doi.org/10.21273/HORTSCI.35.5.885.

Farquhar GD, Sharkey TD. 1982. Stomatal conductance and photosynthesis. Annu Rev Plant Physiol. 33(1):317–345. https://doi.org/10.1146/annurev.pp.33.060182.001533.

Gu JF, Zhou ZX, Li ZK, Chen Y, Wang ZQ, Zhang H. 2017. Rice (*Oryza sativa* L.) with reduced chlorophyll content exhibit higher photosynthetic rate and efficiency, improved canopy light distribution, and greater yields than normally pigmented plants. Field Crops Res. 200:58–70. https://doi.org/10.1016/j.fcr.2016.10.008.

Hu C, Elias E, Nawrocki WJ, Croce R. 2023. Drought affects both photosystems in Arabidopsis thaliana. New Phytol. 240(2):663–675. https://doi.org/10.1111/nph.19171.

Huang XJ, Xu ZH, Niu RM, Shen T, Chen WP. 2020. Effect of etiolation on photosynthesis and chlorophyll fluorescence 'Cabernet Sauvignon' grapes. Non-wood Forest Res. 38(03):190–199. https://doi.org/10.14067/j.cnki.1003-8981.2020.03.022.

Ji SJ, Zhang YF, Xu MH, Zhao MR, Chen HX, Lu YG, Pang SQ, Xu W. 2024. Characterization of low-temperature sensitivity and chlorophyll fluorescence in yellow leaf mutants of tomato. Agronomy. 14(10):2382. https://doi.org/10.3390/agronomy14102382.

Jia M, Li D, Colombo R, Wang Y, Wang X, Cheng T, Zhu Y, Yao X, Xu C, Ouer G, Li H, Zhang C. 2019. Quantifying chlorophyll fluorescence parameters from hyperspectral reflectance at the leaf scale under various nitrogen treatment regimes in winter wheat. Remote Sensing. 11(23):2838. https://doi.org/10.3390/rs11232838.

Jiang YW, Wu MF, Li YL, Luo J, Shen TJ, Qiao G. 2022. Photosynthetic characteristics and mineral nutrition of different degrees of yellowing leaves of 'Manaohong' cherry. North Hortic. (12):47–51. https://doi.org/10.11937/bfyy.20194183.

Lawlor DW. 2002. Limitation to photosynthesis in water-stressed leaves: Stomata vs. metabolism and the role of ATP. Ann Bot. 89(7):871–885. https://doi.org/10.1093/aob/mcf110.

Lecoq H, Bourdin D, Wipf-Scheibel C, Bon M, Lot H, Lemaire O, Herrbach E. 1992. A new yellowing disease of cucurbits caused by a luteo virus, cucurbit apbid-borne yellows virus. Plant Pathol. 41(6):749–761. https://doi.org/10.1111/j.1365-3059.1992.tb02559.x.

Lee J-A, Choi S-K, Yoon J-Y, Hong J-S, Ryu K-H, Lee S-Y, Choi J-K. 2007. Variation in the pathogenicity of lily isolates of cucumber mosaic virus. Plant Pathol J. 23(4):251–259. https://doi.org/10.5423/PPJ.2007.23.4.251.

Li B, Zhang J, Tian P, Gao X, Song X, Pan X, Wu Y. 2024. Cytological, physiological, and transcriptomic analyses of the leaf color mutant yellow leaf 20 (*yl20*) in eggplant (*Solanum melongena* L.). Plants. 13(6):855. https://doi.org/10.3390/plants13060855.

Li M, Li W, Sun Y, Mao P, Qi X, Wang Y. 2018. Analysis of leaf tissue structures between rust-resistant and rust-susceptible Zoysia grass (*Zoysia japonica*). Acta Physiol Plant. 40(4):1–9. https://doi.org/10.1007/s11738-018-2643-6.

Liu J, Wang J, Yao X, Zhang Y, Li J, Wang X, Xu Z, Chen W. 2015. Characterization and fine mapping of thermo-sensitive chlorophyll deficit mutant1 in rice (*Oryza sativa* L.). Breed Sci. 65(2):161–169. https://doi.org/10.1270/jsbbs.65.161.

Liu ZJ, Wu YX, Xiang YS, Zhao Y, Yin WJ, Ma XQ, He TM. 2014. Effects of physiological iron deficiency on leaf anatomical structure of Korla fragrant pear. J Xinjiang Agric Univ. 37(03):203–208. https://doi:10.3969/j.issn.1007-8614.2014.03.006.

Liu WG, Wang F, Zhao Q. 2018. Effects of different fertilizers on control of kiwifruit etiolated disease and yield. Anhui Agric Sci. 46(27):

154–156 + 165. https://doi.org/10.13989/j.cnki.0517-6611.2018.27.044.
Liu KQ, Jia ZF, Liang GL, Liu Y, Ma X, Liu WH. 2022. Response of chlorophyll synthesis and fluorescence characteristics of oat seedling to soil drought. Pratacutural Sci. 39(6):1165–1175. https://doi.org/10.11829/j.issn.1001-0629.2021-0366.
Luo T, Wu JM, Yan HF, Deng YC, Lakshmanan P, Qiu LH, Chen RF, Fan YG, Zhou HW, Huang KJ, Huang X, Zhou ZF. 2022. Control effect and cost analysis of different soil conditioner (fertilizers) on ratoon chlorosis of sugarcane. Southwest China J Agric. 35(03):564–570. https://doi.org/10.16213/j.cnki.scjas.2022.3.012.
Lv M, Liu HH, Mao HD, Zhao QR, Zhao HX, Hu SW. 2010. Changes of chlorophyll synthesis metabolism in chlorophyll-deficient mutant in *Brassica juncea*. Northwest Bot J. 30(11):2177–2183.
Malapascua J, Jerez CG, Sergejevova M, Figueroa FL, Masojidek J. 2014. Photosynthesis monitoring to optimize growth of microalgal mass cultures: Application of chlorophyll fluorescence techniques. Aquat Biol. 22:123–140. https://doi.org/10.3354/ab00597.
Maust BE, Espadas F, Talavera C, Aguilar M, Santamaria JM, Oropeza C. 2003. Changes in carbohydrate metabolism in coconut palms infected with the lethal yellowing phytoplasma. Phytopathology. 93(8):976–981. https://doi.org/10.1094/PHYTO.2003.93.8.976.
Motohashi R, Myouga F. 2015. Chlorophyll fluorescence measurements in *Arabidopsis* plants using a pulse-amplitude modulated (PAM) fluorometer. Bio-protocol. 5(9):e1532. https://doi.org/10.21769/BioProtoc.1532.
Navas-Castillo J, Camero R, Bueno M, Moriones E. 2000. Severe yellowing outbreaks in tomato in Spain associated with infections of tomato chlorosis virus. Plant Dis. 84(8):835–837. https://doi.org/10.1094/PDIS.2000.84.8.835.
Niimi Y, Han DS, Mori S, Kobayashi H. 2003. Detection of cucumber mosaic virus, lily symptomless virus and lily mottle virus in *Lilium* species by RT-PCR technique. Sci Hortic. 97(1):57–63. https://doi.org/10.1016/S0304-4238(02)00125-5.
Ort DR, Merchant SS, Alric J, Barkan A, Blankenship RE, Bock R, Croce R, Hanson MR, Hibberd JM, Long SP, Moore TA, Moroney J, Niyogi KK, Parry MAJ, Peralta-Yahya PP, Prince RC, Redding KE, Spalding MH, Van Wijk KJ, Vermaas WFJ, von Caemmerer S, Weber APM, Yeates TO, Yuan JS, Zhu XG. 2015. Redesigning photosynthesis to sustainably meet global food and bioenergy demand. Proc Natl Acad Sci USA. 112(28):8529–8536. https://doi.org/10.1073/pnas.1424031112.
Prakash JS, Baig MA, Mohanty P. 2001. Senescence induced structural reorganization of thylakoid membranes in *Cucumis sativus* cotyledons; LHC II involvement in reorganization of thylakoid membranes. Photosynth Res. 68(2):153–161. https://doi.org/10.1023/A:1011876412537.
Rascher U, Liebig M, Lüttge U. 2000. Evaluation of instant light-response curves of chlorophyll fluorescence parameters obtained with a portable chlorophyll fluorometer on site in the field. Plant Cell Environ. 23(12):1397–1405. https://doi.org/10.1046/j.1365-3040.2000.00650.x.
Reinbothe S, Reinbothe C. 1996. Regulation of chlorophyll biosynthesis in angiosperms. Plant Physiol. 111(1):1–7. https://doi.org/10.1104/pp.111.1.1.
Roy SJ, Regon P, Tanti B. 2024. Morpho-physiochemical responses of *Capsicum chinense* Jacq. (Bhut Jolokia) under different abiotic stresses. Vegetos. 37(5):1817–1832. https://doi.org/10.1007/s42535-024-00825-3.
Rüdiger W. 1997. Chlorophyll metabolism: From outer space down to the molecular level. Phytochemistry. 46(7):1151–1167. https://doi.org/10.1016/S0031-9422(97)80003-9.
Sairam RK, Srivastava GC. 2002. Changes in antioxidant activity in sub-cellular fractions of tolerant and susceptible wheat genotypes in response to long term salt stress. Plant Sci. 162(6):897–904. https://doi.org/10.1016/S0168-9452(02)00037-7.
Schelbert S, Aubry S, Burla B, Agne B, Kessler F, Krupinska K, Hörtensteiner S. 2009. Pheophytin pheophorbide hydrolase (pheophytinase) is involved in chlorophyll breakdown during leaf senescence in Arabidopsis. Plant Cell. 21(3):767–785. https://doi.org/10.1105/tpc.108.064089.
Shao G, Liu R, Qian Z, Zhang H, Hu Q, Zhu Y, Chen S, Chen F, Jiang J, Wang L. 2022. Transcriptome analysis reveals genes respond to chlorophyll deficiency in green and yellow leaves of *Chrysanthemum morifolium* ramat. Horticulturae. 8(1):14. https://doi.org/10.3390/horticulturae8010014.
Shahsavandi F, Eshghi S, Gharaghani A, Ghasemi-Fasaei R, Jafarinia M. 2020. Effects of bicarbonate induced iron chlorosis on photosynthesis apparatus in grapevine. Sci Hortic. 270:109427. https://doi.org/10.1016/j.scienta.2020.109427.
Smith MD, Licatalosi DD, Thompson JE. 2000. Co-association of cytochrome f catabolites and plastid-lipid-associated protein with chloroplast lipid particles. Plant Physiol. 124(1):211–221. https://doi.org/10.1104/pp.124.1.211.
Sun WW, Meng XM, Xu XY, Wu MH, Qing MY, Lin MM, Zhang XY, Yue GZ. 2020. Bull Bot Res. 40(03):321–329. https://doi.org/10.7525/j.issn.1673-5102.2020.03.001.
Tan J, Zhang T, Xia S, Yan M, Li F, Sang X, He G, Ling Y. 2019. Fine mapping of a novel yellow-green leaf 14 (*ygl14*) mutant in rice. Euphytica. 215(5):100. https://doi.org/10.1007/s10681-019-2424-3.
Tanaka A, Tanaka R. 2006. Chlorophyll metabolism. Curr Opin Plant Biol. 9(3):248–255. https://doi.org/10.1016/j.pbi.2006.03.011.
Tang N, Jia RL, Yin JC, Wang Y, Tang DC. 2021. Effects of cold treatments on seedling emergence and growth of *Lilium davidii* var. *unicolor* bulblets. HortScience. 56(9):1119–1124. https://doi.org/10.21273/HORTSCI15951-21.
Tripathy BC, Pattanayak GK. 2012. Chlorophyll biosynthesis in higher plants. Springer, Dordrecht, Netherlands. 34: 63–94. https://doi.org/10.1007/978-94-007-1579-0_3.
Vacek S, Hejcman M, Semelová V, Remeš J, Podrázský V. 2009. Effect of soil chemical properties on growth, foliation and nutrition of Norway spruce stand affected by yellowing in the Bohemian Forest Mts. Czech Republic. Eur J Forest Res. 128(4):367–375. https://doi.org/10.1007/s10342-009-0272-8.
Wang CX, Tian WW, Tian M, OuYang T, Wang FZ. 2013. The preliminary study of xantha mutants in Oncidium. J Nucl Agric Sci. 27(12):1845–1852.
Wang GJ, Zeng FL, Peng S, Sun B, Wang Q, Wang JY. 2022. Effects of reduced chlorophyll content on photosystem functions and photosynthetic electron transport rate in rice leaves. J Plant Physiol. 272:153669. https://doi.org/10.1016/j.jplph.2022.153669.
Wang JY, Shen JS, Gu MM, Wang J, Cheng TR, Pan HT, Zhang QX. 2017. Leaf coloration and photosynthetic characteristics of hybrids between *Forsythia* 'Courtaneur' and *Forsythia koreana* 'Suwon Gold'. HortScience. 52(12):1661–1667. https://doi.org/10.21273/HORTSCI12177-17.
Wang S, Wang P, Gao L, Yang R, Li L, Zhang E, Wang Q, Li Y, Yin Z. 2017. Characterization and complementation of a chlorophyll-less dominant mutant GL1 in *Lagerstroemia indica*. DNA Cell Biol. 36(5):354–366. https://doi.org/10.1089/dna.2016.3573.
Wang ZJ, Xie ZM, Tian YS, Chen L, Dong YM, Li YZ, Lv ZZ. 2015. Analysis of photosynthetic characteristics and chlorophyll fluorescence kinetic parameters of rice yellowish leaves under condition of drip irrigation with plastic film mulching. Acta Agric Boreali-occidentalis Sinica. 24(02):59–65. https://doi.org/10.7606/j.issn.1004-1389.2015.02.011.
Willits D, Peet M. 1999. Using chlorophyll fluorescence to model leaf photosynthesis in greenhouse pepper and tomato. Acta Hortic. 507:311–317. https://doi.org/10.17660/ActaHortic.1999.507.36.
Wu X, Mao XJ, Fan LL, Chen LY, He TY, Rong JD, Zheng YS. 2022. Photosynthetic characteristics of different color leaves of *Schefflera odorata* 'Variegate'. Chin J Trop Crops. 43(03):556–564. https://doi.org/doi:10.3969/j.issn.1000-2561.2022.03.014.
Wu ZM, Zhang X, He B, Diao LP, Sheng SL, Wang JL, Guo XP, Su N, Wang LF, Jiang L, Wang CM, Zhai HQ, Wan JM. 2007. A Chlorophyll-deficient rice mutant with impaired chlorophyllide esterification in chlorophyll biosynthesis. Plant Physiol. 145(1):29–40. https://doi.org/10.1104/pp.107.100321.
Xiao HG, Yang HW, Rao Y, Yang B, Zhu Y, Zhang WL. 2013. Analysis of chloroplast ultrastructure, stomatal characteristic parameters and photosynthetic characteristics of chlorophyll reduced mutant in *Brassica napus* L. Sci Agric Sin. (4):715–727. https://doi.org/10.3864/j.issn.0578-1752.2013.04.006.
Xu B, Zhang C, Gu Y, Cheng R, Huang D, Liu X, Sun Y. 2023. Physiological and transcriptomic analysis of a yellow leaf mutant in watermelon. Sci Rep. 13(1):9647. https://doi.org/10.1038/s41598-023-36656-6.
Yang XM, Wu XL, Liu YF, Li TL, Qi MF. 2018. Analysis of chlorophyll and photosynthesis of a tomato chlorophyll-deficient mutant induced by EMS. J Appl Ecol. 29(6):1983–1989. https://doi.org/10.13287/j.1001-9332.201806.021.
You XJ, Xie CY, Liu KL, Gu ZX. 2010. Isolation of non-starch polysaccharides from bulb of tiger lily (*Lilium lancifolium* Thunb.) with fermentation of *Saccharomyces cerevisiae*. Carbohydrate Polymers. 81(1):35–40. https://doi.org/10.1016/j.carbpol.2010.01.051.
Yu M, Hu CX, Wang YH. 2006. Effects of molybdenum on the intermediates of chlorophyll biosynthesis in winter wheat cultivars under low temperature. J Integr Agric. 5(9):670–677. https://doi.org/10.1016/S1671-2927(06)60109-0.
Zeng XX, Li SR, Liu YJ, Yu XF. 2024. Study on the physiological basis of the formation of white-green mosaic leaves of *Iris ensata* 'Variegata'. J Sichuan Agric Univ. 42(04):871–878. https://doi.org/10.16036/j.issn.1000-2650.202309389.
Zhang CY, Wang MH, Gao XZ, Guo SN, Li J, Lin HY, Liu QR, Shen CW. 2019. Photosynthetic physiological and histology in novel etiolated branch of the 'Xiangfeicui' tea plant (*Camellia sinensis*). Mol Plant Breed. 17(23):7892–7900. https://doi.org/10.13271/j.mpb.017.007892.

Zhang H, Zhang W, Xiang F, Zhang Z, Guo Y, Chen T, Duan F, Zhou Q, Li X, Fang M, Li X, Li B, Zhao X. 2023. Photosynthetic characteristics and genetic mapping of a new yellow leaf mutant *crm1* in *Brassica napus*. Mol Breed. 43(11):80. https://doi.org/10.1007/s11032-023-01429-6.

Zhang J, Gao YX, Zhou XJ, Hu LP, Xie TZ. 2010. Chemical characterisation of polysaccharides from *Lilium davidii*. Nat Prod Res. 24(4):357–369. https://doi.org/10.1080/14786410903182212.

Zhang M, Shen J, Wu Y, Zhang X, Zhao Z, Wang J, Cheng T, Zhang Q, Pan H. 2022. Comparative transcriptome analysis identified ChlH and POLGAMMA2 in regulating yellow-leaf coloration in *Forsythia*. Plant Sci. 13:1009575. https://doi.org/10.3389/fpls.2022.1009575.

Zhang Q, Zhang M, Ding Y, Zhou P, Fang YM. 2018. Composition of photosynthetic pigments and photosynthetic characteristics in green and yellow sectors of the variegated *Aucuba japonica* 'Variegata' leaves. Flora. 40:25–33.

Zhang YB, Wang YJ, Meng J, Xie ZK, Wang RY, Hadley RK, Guo ZH. 2015. Development of an immunochromatographic strip test for rapid detection of lily symptomless virus. J Virol Methods. 220:13–17. https://doi.org/10.1016/j.jviromet.2015.03.021.

Zhong HQ, Lin RY, Wu JS, Lin B, Ye XX. 2021. Physiological, biochemical and cell structure analysis of leaf mutant traits in *Cymbidium* hybrid 'Purple Element'. Acta Botanica Boreali-Occidentalia Sinica. 41(07): 1165–1174.